

## Electron energy levels in GaAs-Ga<sub>1-x</sub>Al<sub>x</sub>As heterojunctions

Frank Stern

IBM Thomas J. Watson Research Center, Yorktown Heights, New York 10598

Sankar Das Sarma

IBM Thomas J. Watson Research Center, Yorktown Heights, New York 10598  
and Department of Physics and Astronomy, University of Maryland, College Park, Maryland 20742\*

(Received 31 January 1984)

Calculated results for energy levels of electrons in GaAs-Ga<sub>1-x</sub>Al<sub>x</sub>As heterojunctions are presented and their sensitivity to various parameters—including acceptor doping level in the GaAs, heterojunction barrier height, effective-mass and dielectric-constant discontinuities, interface grading, and ambient temperature—is examined.

### I. INTRODUCTION

Interest in the properties of electrons in GaAs-Ga<sub>1-x</sub>Al<sub>x</sub>As heterojunctions has led to a number of calculations<sup>1-3</sup> of their energy levels and other electronic properties. In this paper, calculated results of energy levels are presented for a range of temperatures and material parameters, including interface grading, which has not been treated in detail previously (however, see Price and Stern<sup>4</sup>). Values of the energy levels and of the Fermi level are needed to find the charge transfer from donors in the Ga<sub>1-x</sub>Al<sub>x</sub>As to the GaAs channel. Energy-level differences are more closely related to subband spectroscopy and to the onset of intersubband scattering. We find that the energy levels are affected to varying degrees by the values of the parameters, and that differences between them are affected less. The differences are most sensitive to the acceptor doping level in the GaAs. Many aspects of the calculations presented here have counterparts in calculations for silicon inversion layers and related two-dimensional electron systems, which have been reviewed by Ando *et al.*<sup>5</sup>

The next two sections give a description of the calculation, which follows familiar lines except for the treatment of the graded interface, and a discussion of the density-functional scheme that is used to take electron-electron interactions into account approximately. Section IV gives results of the calculations and Sec. V gives discussion and conclusions. A preliminary account of this work, but without electron-electron interaction effects, was presented last year (see Ref. 6).

### II. OUTLINE OF THE CALCULATION

The conduction-band edge in a heterojunction, illustrated in Fig. 1(a), has a spatial dependence both because of electrostatic potentials and because of the energy-band discontinuity associated with the change in material across the heterojunction. In this calculation the heterojunction effect is modeled using a graded interface in which the barrier height as well as the effective mass and dielectric constant are assumed to change smoothly in a

transition layer whose thickness is specified. A physical interface between two materials may be crystallographically abrupt, but the bonding environment of the atoms adjoining this interface will change on at least an atomic scale. In place of a microscopic model of this transition, we use an approximate treatment in which the parameters vary smoothly but rapidly. A similar calculation has been used to treat the energy levels of electrons on the surface of liquid helium.<sup>7</sup>

An electron moves in an effective potential given by

$$V(z) = -e\phi(z) + V_h(z) + V_{xc}(z) + V_{im}(z), \quad (1)$$

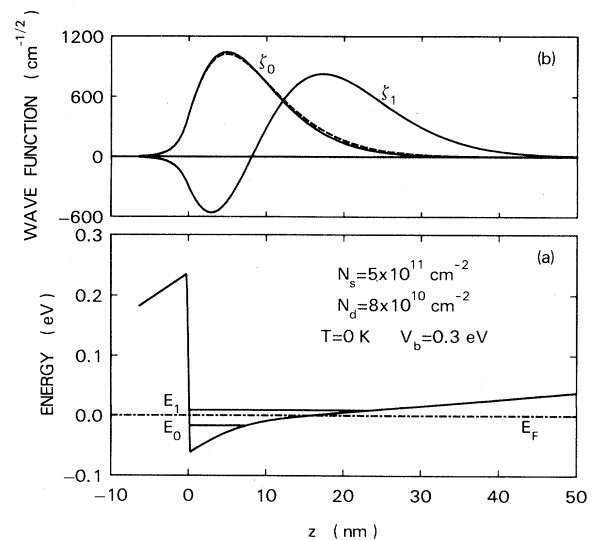


FIG. 1. (a) Conduction-band edge vs distance from a GaAs-Ga<sub>0.7</sub>Al<sub>0.3</sub>As heterojunction with  $5 \times 10^{11} \text{ cm}^{-2}$  electrons in the GaAs channel, an acceptor doping of  $3 \times 10^{14} \text{ cm}^{-3}$  in the GaAs, and a barrier height of 0.3 eV.  $E_0$  and  $E_1$  label the bottoms of the lowest and of the first excited subbands, respectively. All energies in this figure are relative to the Fermi energy  $E_F$ . (b) Normalized envelope wave functions (solid curves)  $\xi_0(z)$  and  $\xi_1(z)$  for electrons in the two lowest subbands calculated with inclusion of exchange and correlation effects. The dashed curve gives  $\xi_0(z)$  calculated without including exchange and correlation effects.

where  $\phi(z)$  is the electrostatic potential,  $V_h(z)$  is the effective potential energy associated with the (graded) heterojunction discontinuity,  $V_{xc}(z)$  is the local exchange-correlation potential energy described in the next section, and  $V_{im}(z)$  is the image potential energy. The normalized envelope function  $\xi_i(z)$  for an electron in subband  $i$  is assumed to be given by a Schrödinger equation of the BenDaniel-Duke<sup>8</sup> form:

$$-\frac{\hbar^2}{2} \frac{d}{dz} \frac{1}{m(z)} \frac{d\xi_i(z)}{dz} + V(z)\xi_i(z) = E_i \xi_i(z), \quad (2)$$

where  $m(z)$  is the position-dependent effective mass and  $E_i$  is the energy of the bottom of the  $i$ th subband. Some or all of the energy levels correspond to states that can penetrate the barrier into lower-energy regions in the Ga<sub>1-x</sub>Al<sub>x</sub>As and thus can be affected by the potential profile there, a situation treated by Vinter.<sup>2</sup> This does not have significant consequences for the heterojunctions in equilibrium treated here but is important for states whose energies lie near the top of the heterojunction barrier or when a current is flowing across the heterojunction.

Poisson's equation for the electrostatic potential (in SI units) takes the form

$$\frac{d}{dz} \epsilon_0 \kappa(z) \frac{d\phi(z)}{dz} = e \sum N_i \xi_i^2(z) - \rho_I(z), \quad (3)$$

$$N_i = \frac{m_c k_B T}{\pi \hbar^2} \ln \left[ 1 + \exp \left[ \frac{E_F - E_i}{k_B T} \right] \right], \quad (4)$$

where  $\kappa(z)$  is the position-dependent dielectric constant,

$$G(z) = \begin{cases} (z + z_h)/z_t, & 0 < z < z_h - a_t, \\ \frac{\{z + 3z_h - a_t + (2a_t/\pi) \cos[\pi(z - z_h)/2a_t]\}}{2z_t}, & z_h - a_t < z < z_h + a_t, \\ 1, & z > z_h + a_t, \\ 1 - G(-z), & z < 0, \end{cases} \quad (6)$$

where  $V_b$  is the barrier height,  $z_t$  and  $a_t$  are parameters that characterize the transition layer ( $z_t \geq 2a_t > 0$ ), and  $z_h = z_t/2$ . The nominal thickness of the transition layer is  $z_t + a_t$ . The two remaining graded quantities are found similarly, using  $G(z)$  to interpolate between the value in the Ga<sub>1-x</sub>Al<sub>x</sub>As and the value in the GaAs.

The image potential energy  $V_{im}$  is obtained from the graded dielectric constant using the method described in Ref. 7, and, as was intended, avoids the singularity of the conventional result

$$V_{im}(z) = \begin{cases} [(\kappa_c - \kappa_b) e^2] / [16\pi\epsilon_0\kappa_c(\kappa_c + \kappa_b)z], & z > 0 \\ [(\kappa_c - \kappa_b) e^2] / [16\pi\epsilon_0\kappa_b(\kappa_c + \kappa_b)z], & z < 0 \end{cases} \quad (7)$$

at the interface,  $z=0$ . The result in Eq. (7) cannot be used directly in the effective-mass Schrödinger equation, Eq. (2), when there is a finite barrier height because a finite value of the envelope wave function at the interface leads to a nonintegrable singularity in the energy. Most authors

$N_i$  is the number of electrons per unit area in subband  $i$ ,  $E_F$  is the Fermi energy, and  $m_c$  is the effective mass in the GaAs.<sup>9</sup> The potential is taken to be 0 at the interface and its derivative is taken to be 0 in the GaAs bulk. The impurity charge density in the GaAs ( $z > 0$ ) is taken to be  $\rho_I(z) = -eN_{Ac}$ , where  $N_{Ac}$  is the net acceptor density in the GaAs, and is here taken to vanish in the Ga<sub>1-x</sub>Al<sub>x</sub>As ( $z < 0$ ). Subscript  $c$  generally denotes the GaAs (channel) side of the heterojunction, and subscript  $b$  denotes the Ga<sub>1-x</sub>Al<sub>x</sub>As (barrier) side.

Three parameters in the theory change across the heterojunction: the effective heterojunction potential energy  $V_h(z)$ , the effective mass  $m$ , and the dielectric constant  $\kappa$ . The barrier  $V_b$  appears on the Ga<sub>1-x</sub>Al<sub>x</sub>As side of the heterojunction and vanishes on the GaAs side. Since the length scale of the system is given by atomic sizes, a mathematically abrupt transition is unphysical and, as noted below, can lead to mathematical difficulties. To smooth this transition we take a grading function that basically interpolates linearly between the values in the materials bounding the heterojunction, but has rounded corners. This functional form is the same as the one that was used to calculate the energy levels of electrons on the surface of liquid helium,<sup>10</sup> whose density is known to vary from its bulk value to the (very small) value in the vapor in a distance of order 1 nm. Other grading functions would presumably give comparable results. The grading of the interface barrier is taken to be

$$V_h(z) = [1 - G(z)]V_b, \quad (5)$$

avoid this problem by assuming an infinite barrier, as for the Si-SiO<sub>2</sub> interface,<sup>5</sup> or by ignoring the dielectric-constant change. One of the goals of the present calculation is to assess the magnitude of the error made in ignoring the dielectric-constant step.

Apart from the grading effects just noted, the calculation is conventional and will not be described further. In the next section the considerations that enter in a choice of the effective exchange-correlation potential are described.

### III. EXCHANGE-CORRELATION EFFECTS

In this section we first describe the local-density-functional approximation for exchange-correlation effects—the effects of electron-electron interaction beyond the Hartree approximation—and then discuss some of the ways in which this approximation might be improved in connection with heterojunction calculations. A simple way of including many-body exchange-correlation effects

in the calculation of electronic structure is the density-functional method<sup>11</sup> due to Hohenberg, Kohn, and Sham. This method has been used with great success in calculating the electronic structure of atoms, molecules, and solids.<sup>12</sup> The density-functional technique has also been applied quite successfully by Ando<sup>13</sup> and by Das Sarma and Vinter<sup>14</sup> in calculating the electronic subband structure of silicon inversion layers in Si-SiO<sub>2</sub> metal-oxide-semiconductor—field-effect-transistor systems.

Within the density-functional formalism, the electronic energy levels (including exchange-correlation effects) are obtained from the one-electron Kohn-Sham equation<sup>11</sup> which is formally the same as the Schrödinger equation for the Hartree problem except that an additional term, the so-called exchange-correlation potential energy  $V_{xc}$  first introduced by Kohn and Sham,<sup>11</sup> appears in the potential energy. The one-electron wave functions  $\zeta_i(z)$  and energy levels  $E_i$  are usually identified as the real wave functions and energy levels of the system even though the theory is rigorously valid only for the total ground-state energy and density of the system. For justification of this identification we refer the reader to Ando's work<sup>13</sup> on silicon space-charge layers and to von Barth's recent investigation<sup>15</sup> of a more general nature.

The exchange-correlation potential energy  $V_{xc}(z)$  is, in general, an unknown functional<sup>11</sup> of the electron density  $n(z)$ , given by the sum on the right-hand side in Eq. (3).<sup>16</sup> In reality, however, the simplest approximation to the exchange-correlation potential, the so-called local-density-functional approximation, works surprisingly well.<sup>12-15</sup> In this approximation one takes  $V_{xc}(z) \equiv V_{xc}\{n(z)\} \equiv \mu_{xc}[n_0 = n(z)]$ , where  $\mu_{xc}$  is the exchange-correlation contribution to the chemical potential of a homogeneous electron gas having a uniform electron density  $n_0$  which is equal to the local electron density  $n(z)$  of the inhomogeneous system.  $V_{xc}$ , calculated within the local-density-functional approximation, has been parametrized by a number of authors<sup>17</sup> and different forms of  $V_{xc}$  give similar quantitative results for the subband energy levels. We therefore use the simple analytic parametrization<sup>18</sup> suggested by Hedin and Lundqvist:

$$V_{xc}(z) = -[1 + 0.7734x \ln(1 + x^{-1})](2/\pi\alpha r_s) \text{Ry}^*, \quad (8)$$

where  $\alpha = (4/9\pi)^{1/3}$ ,  $x \equiv x(z) = r_s/21$ ,

$$r_s \equiv r_s(z) = \left[ \frac{4}{3} \pi a^* n(z) \right]^{-1/3}, \quad (9)$$

$$a^* = \frac{4\pi\epsilon_0\hbar^2}{me^2}, \quad (10)$$

$\kappa \equiv \kappa(z)$  is the local dielectric constant, and  $m \equiv m(z)$  is the local effective mass. The unit of energy in Eq. (8) is the effective Rydberg,  $\text{Ry}^* = (e^2/8\pi\epsilon_0\kappa a^*)$ , which is approximately 5 meV for GaAs.

One of the problems in applying the local-density-functional formalism to the calculation of the electronic structure of space-charge layers at semiconductor interfaces is that one is working within the effective-mass formalism and hence the corresponding homogeneous electron-gas calculation to obtain  $V_{xc}$  must somehow reflect the dielectric discontinuity at the interface. This is essential<sup>13,14</sup> for the Si-SiO<sub>2</sub> system where the static

dielectric constants for Si and SiO<sub>2</sub> are 11.5 and 3.9, respectively, giving rise to a substantial image interaction effect. In typical GaAs-Ga<sub>1-x</sub>Al<sub>x</sub>As heterostructures the change in dielectric constant is of order 10% or less and consequently the image interaction is much smaller than the direct Coulomb interaction. Thus it is a good approximation to neglect the image effect in calculating  $V_{xc}$  for the GaAs-Ga<sub>1-x</sub>Al<sub>x</sub>As system.

The formal issue of calculating a correct  $V_{xc}$  (even within the local-density-functional approximation) in the presence of a dielectric discontinuity, as encountered in the GaAs-Ga<sub>1-x</sub>Al<sub>x</sub>As heterojunction, remains open. Neglecting the tailing of the electronic wave function into the Ga<sub>1-x</sub>Al<sub>x</sub>As layer, one can write the electron-electron interaction between two electrons on the GaAs side as

$$v(\vec{r}_1, z_1; \vec{r}_2, z_2) = \frac{e^2}{4\pi\epsilon_0\kappa_1[(\vec{r}_1 - \vec{r}_2)^2 + (z_1 - z_2)^2]^{1/2}} + \frac{(\kappa_1 - \kappa_2)}{4\pi\epsilon_0\kappa_1(\kappa_1 + \kappa_2)} \times \frac{e^2}{[(\vec{r}_1 - \vec{r}_2)^2 + (z_1 + z_2)^2]^{1/2}}, \quad (11)$$

where  $(\vec{r}_1, z_1)$  and  $(\vec{r}_2, z_2)$  with  $\vec{r} \equiv (x, y)$  are the positions of the two electrons and  $\kappa_1$  and  $\kappa_2$  are to be identified with the dielectric constants  $\kappa_c$  and  $\kappa_b$  of GaAs and Ga<sub>1-x</sub>Al<sub>x</sub>As, respectively. Equation (11) defines an interaction that is clearly not translationally invariant, by virtue of the second term (the image term). To circumvent this problem Ando wrote<sup>13</sup>

$$(z_1 + z_2)^2 = (z_1 - z_2)^2 + 4z_1z_2 \approx (z_1 - z_2)^2 + 4z^2, \quad (12)$$

and identified this  $z$  as the same  $z$  defining the local density  $n(z) = n_0$  in the calculation of  $V_{xc}$ . Thus  $V_{xc}$  becomes  $V_{xc}[n(z); z]$ , the explicit  $z$  dependence arising from the image interaction. Once Eq. (12) is put into Eq. (11), the resulting interaction can be used to obtain<sup>13</sup>  $\mu_{xc}$  for given values of  $z$  and  $n(z) = n_0$ . This  $\mu_{xc}$  is taken to be the relevant  $V_{xc}$  for the problem.

This particular way of handling the dielectric discontinuity works very well<sup>13,14</sup> for the Si-SiO<sub>2</sub> space-charge layer system, where the potential barrier at the interface is so large that electrons are confined in the Si with almost no effective wave-function tailing into the SiO<sub>2</sub> layer. It is, however, not obvious that this technique can be successfully used in a heterostructure with a dielectric discontinuity where wave-function tailing into the insulating layer is not negligible. The practical problem is that the form of the electron-electron interaction  $v(\vec{r}_1, z_1; \vec{r}_2, z_2)$  now depends specifically on where the electrons are found (i.e., the formula for  $v$  depends on whether both electrons have  $z > 0$  or  $z < 0$  or whether they are on opposite sides of the interface). For the GaAs-Ga<sub>1-x</sub>Al<sub>x</sub>As system these image effects can safely be ignored because the dielectric constants differ so little. In an actual microscopic calculation (i.e., without the effective-mass approximation), this problem would not arise because the microscopic Coulomb interaction is well

defined and translationally invariant everywhere. However, a microscopic calculation for this system may be prohibitively difficult for computational reasons.

Having a graded interface (i.e., going from  $\kappa_1$  to  $\kappa_2$  in a smooth fashion) helps one in defining a local dielectric constant  $\kappa \equiv \kappa(z)$  and effective mass  $m \equiv m(z)$ , so that Eqs. (8)–(10) can be evaluated at each  $z$  without any discontinuity. However, the formal problem (when  $\kappa_1$  and  $\kappa_2$  are very different) of the image effect and the consequent lack of translational invariance in the electron-electron interaction still remains and should be investigated theoretically. The rapid variation of the effective mass in going from the  $\kappa_1$  side of the interface to the  $\kappa_2$  side also raises fundamental questions about the validity of the density-functional scheme as applied within the effective-mass approximation. This variation in the effective mass is handled simply by using the local effective mass in Eqs. (8)–(10). The validity of this approach in defining  $V_{xc}$  is unclear, but the graded-interface approximation may lead to errors even in the Hartree approximation and these are likely to overshadow the effects of grading on the exchange-correlation potential.

The finite-temperature generalization of the local-density-functional approximation to the electronic structure of space-charge layers has been investigated in detail by Das Sarma and Vinter<sup>14</sup> in the context of silicon inversion layers. Their basic conclusions should be valid for the GaAs heterostructure systems as well. Das Sarma and Vinter found that one can neglect the explicit temperature dependence of  $V_{xc}$ , keeping only the implicit temperature dependence which arises because  $n(z)$  depends on temperature through the occupations of the self-consistent energy levels of the system. Unlike Si inversion layers where different subband ladders have different masses and one must do a “valley-polarized” local-density-functional calculation (when subbands in both ladders are occupied by electrons), GaAs is a single-valley isotropic system where the simple unpolarized local-density-functional approximation outlined above is applicable. If one wants to investigate the possibility of a ferromagnetic (or any other spin-related) instability in the GaAs heterostructure, one can readily generalize the formalism given here by using a suitable spin-polarized exchange-correlation potential.<sup>19</sup>

In this work we use the local-density-functional approximation as described above in calculating the electronic subband structure of the GaAs-Ga<sub>1-x</sub>Al<sub>x</sub>As heterojunction system. We use the local dielectric constant  $\kappa \equiv \kappa(z)$  and the local effective mass  $m \equiv m(z)$  in obtaining  $V_{xc}$  given by Eqs. (8)–(10). We neglect image effects in  $V_{xc}$ , which should be a good approximation for the GaAs-Ga<sub>1-x</sub>Al<sub>x</sub>As system because  $\kappa_1 \approx \kappa_2$ .

Finally, it should be emphasized that even though the local-density-functional approximation has had great empirical success in the calculation of electronic structure not only for space-charge layers in semiconductors but also for a wide class of systems including bulk solids, surfaces, atoms, and molecules, the condition for its validity is seldom obeyed in physical systems of interest. In particular, the validity of the local-density-functional approximation requires that the electronic density variation be small over distances of the order of a Fermi wavelength.

In a GaAs-Ga<sub>1-x</sub>Al<sub>x</sub>As heterojunction with an electron density of  $10^{12} \text{ cm}^{-2}$ , the Fermi wavelength is about 25 nm, whereas the typical wave-function width is about 10 nm for the lowest subband. Thus the electron density does not vary slowly on the scale of the Fermi wavelength, invalidating the condition for the local-density-functional approximation. It will therefore be interesting to explore the corrections to the exchange-correlation effects calculated in this paper by going beyond this approximation. We plan to calculate such corrections by using the nonlocal-density-functional scheme<sup>20</sup> recently developed by Langreth and Mehl, which gives improved results for the electronic structure in both atoms<sup>20</sup> and solids<sup>21</sup> when compared with the local-density-functional approximation.

#### IV. RESULTS

We first give results for a graded GaAs-Ga<sub>1-x</sub>Al<sub>x</sub>As heterojunction at absolute zero for several values of the net acceptor doping level  $N_{Ac}$  in the GaAs. The heterojunction parameters we used are

$$\begin{aligned} x &= 0.3, \quad V_b = 0.3 \text{ eV}, \\ m_c, m_b &= 0.07, \quad 0.088m_0, \\ \kappa_c, \kappa_b &= 13.0, \quad 12.1, \\ z_i, a_i &= 0.4, \quad 0.1 \text{ nm}, \end{aligned} \tag{13}$$

where the last line corresponds to a 0.5-nm interface grading. Calculated energy levels for  $N_{Ac} = 0.01, 0.1, 0.3, 1.0, 3.0,$  and  $10 \times 10^{-15} \text{ cm}^{-3}$ , corresponding to  $N_d = 0.146, 0.46, 0.80, 1.47, 2.56,$  and  $4.69 \times 10^{11}$  depletion charges per  $\text{cm}^2$ , respectively, are shown in Fig. 2. A representative conduction-band profile and the wave function for the lowest subband are shown in Fig. 1 for channel electron density  $N_s = 5 \times 10^{11} \text{ cm}^{-2}$  and  $N_{Ac} = 3 \times 10^{14} \text{ cm}^{-3}$ . The dashed curve in Fig. 1(b) gives the corresponding wave function calculated without the exchange-correlation potential energy  $V_{xc}$  in the effective potential energy of Eq. (1). These results show that the energy levels and energy-level differences are quite sensitive to the acceptor doping density in the GaAs even at densities in the  $10^{14} \text{ cm}^{-3}$  range.

Exchange-correlation effects in the energy levels can be seen from the differences between the solid and dashed curves in Fig. 2, calculated with and without these effects, respectively, for a net GaAs acceptor doping density  $N_{Ac} = 0.3 \times 10^{15} \text{ cm}^{-3}$ . The effects are also clearly seen in Fig. 3, which shows the value of  $N_s$  at which the second subband is just occupied versus the square root of the density of depletion charges  $N_d$ , calculated with and without the exchange-correlation potential. Inclusion of exchange and correlation increases the carrier concentration at which the Fermi level crosses into the second subband by about  $2 \times 10^{11} \text{ cm}^{-2}$  at all values of  $N_d$ , both for AlAs fractions  $x = 0.3$  and  $0.4$  (the larger value of  $x$  is needed for large values of  $N_d$  to keep the electrons in the first excited subband from leaking into the barrier to such an extent that the energy-level calculation is significantly affected). Occupation of the second subband opens a new

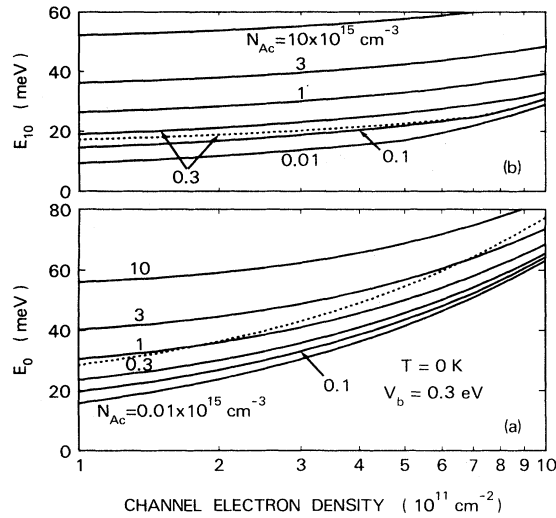


FIG. 2. Calculated values of (a) the energy  $E_0$  of the bottom of the lowest subband and (b) the energy difference  $E_{10}$  between the first excited subband and the lowest subband at absolute zero vs channel electron density  $N_s$  for the six indicated values of net acceptor doping  $N_{Ac}$  in the GaAs. The corresponding values of  $N_d$ , the density of charges in the depletion layer, are 0.146, 0.46, 0.80, 1.47, 2.56, and  $4.69 \times 10^{11} \text{ cm}^{-2}$ , respectively. The dashed curves give the values calculated without inclusion of exchange and correlation effects for  $N_{Ac} = 0.3 \times 10^{15} \text{ cm}^{-3}$ .

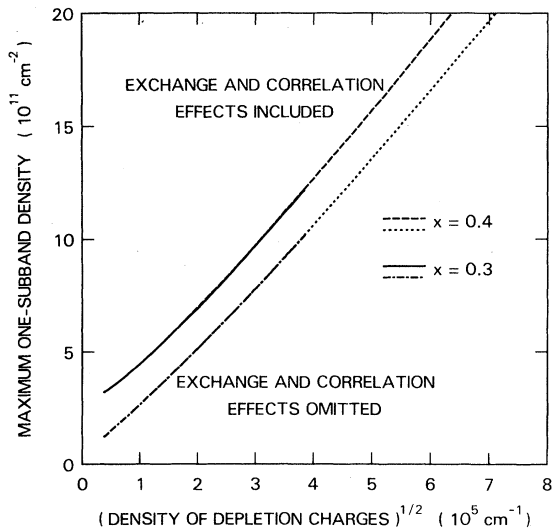


FIG. 3. Channel electron density at which the second subband is just occupied at  $T=0 \text{ K}$  vs the square root of the density of depletion charges  $N_d$ , calculated with (solid and dashed curve) and without (dot-dashed curve and dotted curve) inclusion of the exchange-correlation potential, for GaAs- $\text{Ga}_{1-x}\text{Al}_x\text{As}$  heterojunctions with AlAs fractions  $x$  of 0.3 and 0.4. The results for values of  $N_d$  below about  $10^{10} \text{ cm}^{-2}$  approximate those expected for semi-insulating or  $n$ -type GaAs. Results for the largest values of  $N_d$  are calculated with  $x=0.4$  because the higher barrier reduces electron leakage through the barrier.

scattering channel and lowers the mobility.<sup>22-24</sup> Values of the channel density at the beginning of the occupation of the second subband have been calculated by Ando<sup>1</sup> with and without exchange for two values of  $N_d$ , and by Bastard,<sup>25</sup> using an extension of the Fang-Howard variational wave function in the Hartree approximation, for a range of values of  $N_d$ .

Figure 4 shows how the energy levels change with temperature for several values of  $N_s$  in a heterojunction with net acceptor doping  $N_{Ac} = 3 \times 10^{14} \text{ cm}^{-3}$  in the GaAs. As in the case of silicon inversion layers,<sup>5,26</sup> the subband energies increase with increasing temperature because increasing the temperature increases the occupation of higher subbands, thereby increasing the average electric field in the well.

Some representative values of the average distance

$$z_{av} = N_s^{-1} \int_{-\infty}^{\infty} z \sum N_i \xi_i^2(z) dz \quad (14)$$

of electrons from the interface are shown in Fig. 5. Fractional occupations of the subbands are shown in Fig. 6 and confirm Vinter's<sup>3</sup> finding that most of the channel electrons are in the lowest subband even at room temperature.

An important quantity in determining the transfer of electrons from donor impurities in the  $\text{Ga}_{1-x}\text{Al}_x\text{As}$  to the GaAs channel is the position of the Fermi level relative to the bottom of the GaAs conduction band at the interface. For this purpose we take the Fermi level as found in our calculation and refer it to the extrapolated conduction-band edge at the center of the graded interface layer, ignoring the image and exchange-correlation potentials in the determination of the band edge but not in the energy-level calculation. Values found in this way are given in Fig. 7 for  $T=0, 77,$  and  $300 \text{ K}$ . Also shown is the value estimated for  $0 \text{ K}$  using the triangular-well approximation with the average electric field in the channel, given by  $e(N_d + 0.5N_s)/\epsilon_0\kappa_c$ . This approximation, which ignores

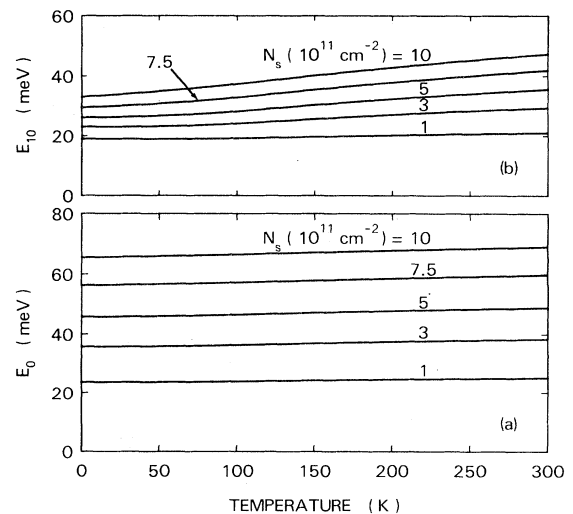


FIG. 4. Temperature dependence of (a) the energy  $E_0$  of the bottom of the lowest subband and (b) the energy difference  $E_{10}$  between the two lowest subbands, for net acceptor doping  $N_{Ac} = 3 \times 10^{14} \text{ cm}^{-3}$  in the GaAs for several values of  $N_s$ , the electron density in the channel.

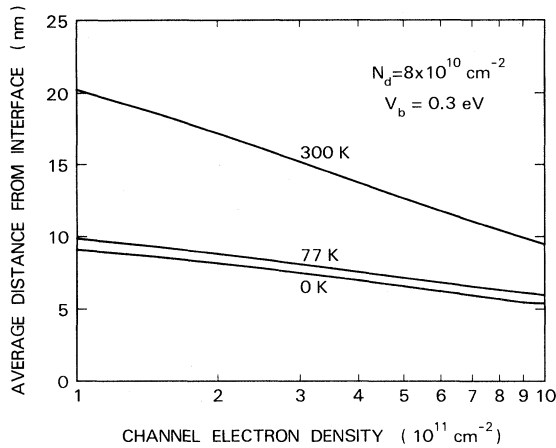


FIG. 5. Average electron distance from the interface,  $z_{av}$ , as a function of channel electron density  $N_s$  for 0, 77, and 300 K for the same acceptor doping as in Fig. 4.

image and exchange-correlation effects, is the one used for the next-to-last row of Table I.

The contribution of the image potential to the energy levels was tested by repeating the calculation with the dielectric constant of the Ga<sub>1-x</sub>Al<sub>x</sub>As taken to be equal to the dielectric constant of the GaAs. The change is so small that it would not be easily visible on a plot of the energies themselves. Therefore, we give in Table I the energy levels calculated with the standard parameters and also with the dielectric constants set equal to each other. As noted before, the image potential cannot be properly included in a calculation for a sharp interface because of the divergence that arises there. The image potential has therefore been omitted in most other heterojunction calculations. Table I shows that this leads to very small errors in the energies.

We can also test the sensitivity of the energy levels to a number of other parameters in the calculation. For these tests, the image potential is omitted. First, we look at the sensitivity of the results to the effective mass in the Ga<sub>1-x</sub>Al<sub>x</sub>As. Table I gives a few representative results for  $m_b = 0.07m_0$  and for the value  $0.088m_0$  used in most of the calculations. Note that the effect on energy-level

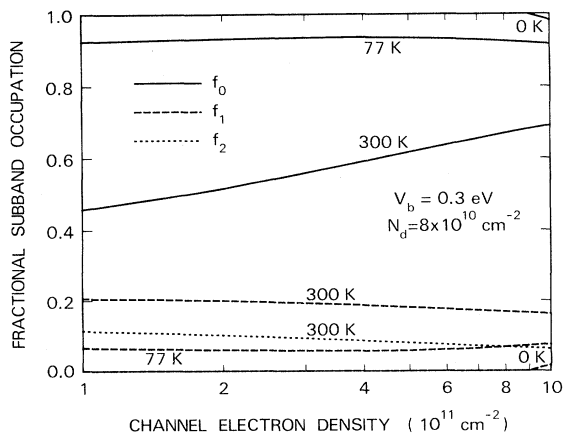


FIG. 6. Fractional occupation  $f_i = N_i/N_s$  of the three lowest subbands vs  $N_s$ . Parameters are the same as for Fig. 5.

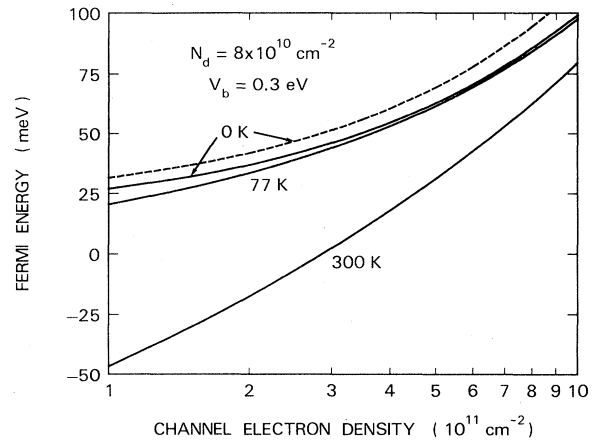


FIG. 7. Calculated Fermi energy relative to the extrapolated conduction-band edge at the interface vs  $N_s$ . Parameters are the same as for Fig. 5. The dashed curve gives the value found using the triangular-well approximation with the average field in the well, as in the next-to-last line of Table I.

differences is smaller than the effect on the individual levels, an example of a general result<sup>26</sup> that small changes in boundary conditions tend to shift levels together (note that here, in contrast to the case of silicon inversion layers, there is only one ladder of levels because there is no valley degeneracy at the bottom of the GaAs conduction band).

The dependence of the energy levels on the thickness  $z_t + a_t$  of the interface transition layer is also given in Table I. The effects are small and again are even smaller for energy-level differences than for the individual energies.

Figure 8 shows the dependence of the energy levels on the fraction  $x$  of AlAs in the barrier. We take the barrier height in eV to be equal to  $x$ , and take the effective mass

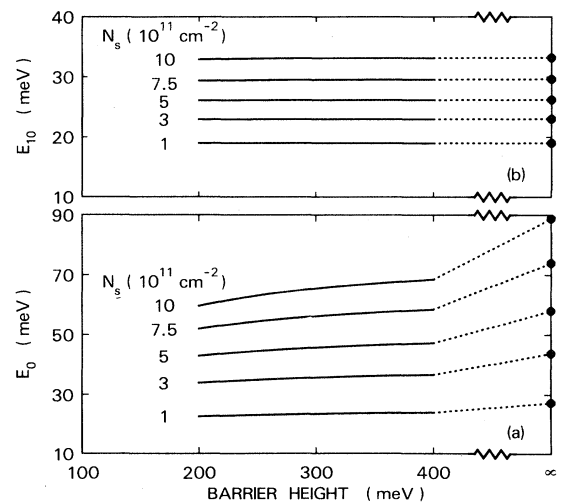


FIG. 8. Dependence of (a) energy levels and (b) energy-level differences on interface barrier height at  $T=0$  K for several values of channel electron density  $N_s$ . The barrier height (in eV) is taken equal to the AlAs fraction  $x$ . See the text for the effective-mass values in the Ga<sub>1-x</sub>Al<sub>x</sub>As. The points at the right edge of the figure are calculated for infinite barrier height. The GaAs acceptor doping is  $N_{Ac} = 3 \times 10^{14} \text{ cm}^{-3}$ .

TABLE I. Some calculated results to show their sensitivity to changes in parameters. The values shown are the first two energy levels,  $E_0$  and  $E_1$ , and their difference  $E_{10}$ , all in meV, and the average distance  $z_0$  (in nm) of electrons in the lowest subband from the GaAs-Ga<sub>1-x</sub>Al<sub>x</sub>As interface for electron densities  $N_s$  of  $10^{11}$  and  $5 \times 10^{11}$  cm<sup>-2</sup>. The “standard” parameter assumptions, used to calculate the values in the first row, are  $T=0$  K, interface barrier height  $V_b=0.3$  eV, dielectric constants  $\kappa_c=13$  and  $\kappa_b=12.1$ , effective masses  $m_c=0.07m_0$  and  $m_b=0.088m_0$ , GaAs net acceptor doping  $N_{Ac}=3 \times 10^{14}$  cm<sup>-3</sup> (for which there are  $N_d=0.8 \times 10^{11}$  charges per cm<sup>2</sup> in the depletion layer), and nominal interface transition layer thickness  $z_t+a_t=0.5$  nm. Exchange and correlation effects are included except where “no xc” is noted. The last three rows give approximate results, without image and exchange-correlation effects, calculated using the triangular-well approximation and the self-consistent variational approximation. More significant figures are given than are warranted by the precision of the calculation, to allow differences to be seen.

Parameter changes	$N_s=1 \times 10^{11}$ cm <sup>-2</sup>				$N_s=5 \times 10^{11}$ cm <sup>-2</sup>			
	$E_0$	$E_1$	$E_{10}$	$z_0$	$E_0$	$E_1$	$E_{10}$	$z_0$
None	23.57	42.55	18.98	9.109	45.72	71.87	26.15	6.586
$\kappa_b=13$ (no image)	23.37	42.40	19.03	9.071	45.40	71.62	26.22	6.565
$\kappa_b=13$ , $m_b=0.07m_0$	23.75	42.77	19.02	9.218	46.49	72.68	26.18	6.696
$\kappa_b=13$ , $z_t+a_t=0$	23.34	42.37	19.03	9.062	45.33	71.56	26.22	6.557
$\kappa_b=13$ , $z_t+a_t=0.15$	23.34	42.37	19.03	9.061	45.32	71.54	26.22	6.555
$\kappa_b=13$ , $z_t+a_t=0.3$	23.35	42.38	19.03	9.064	45.35	71.57	26.22	6.558
$\kappa_b=13$ , $z_t+a_t=0.5$	23.37	42.40	19.03	9.071	45.40	71.62	26.22	6.564
$\kappa_b=13$ , $z_t+a_t=0.7$	23.40	42.43	19.03	9.083	45.49	71.71	26.22	6.575
$\kappa_b=13$ , $z_t+a_t=0.9$	23.44	42.47	19.03	9.099	45.61	71.82	26.21	6.590
No xc	28.47	45.66	17.19	9.346	54.56	77.20	22.64	6.806
$\kappa_b=13$ , $V_b=\infty$ , no xc	32.09	49.33	17.25	10.83	66.68	89.42	22.75	8.336
Triangular well <sup>a</sup>	35.0	61.5	26.5	9.30	76.2	134.1	57.9	6.29
Triangular well <sup>b</sup>	28.1	49.5	21.4	10.36	52.3	93.1	40.7	7.60
Variational <sup>c</sup>	33.1	50.3	17.3	11.56	67.9	93.2	25.3	8.88

<sup>a</sup>Calculated using Eq. (10b) of Ref. 26 with effective field  $F_s=e(N_d+N_s)/\epsilon_0\kappa_c$ .

<sup>b</sup>Calculated as in the previous line, but with  $F_s=e(N_d+0.5N_s)/\epsilon_0\kappa_c$ .

<sup>c</sup>Calculated using Eqs. (15)–(17) of Ref. 26.

in the barrier to be  $m_b/m_0=m_c/m_0+0.06x$ . In the calculations for Fig. 8 we take the interface to be mathematically sharp and therefore set  $\kappa_b=\kappa_c=13$ . The results are shown in Fig. 8 for values of  $x$  from 0.2 to 0.4. Results are also given for infinite barrier height, in which case the results do not depend on the choice of  $m_b$ .

In some experiments it has proved possible to change the channel charge density by applying a voltage to an electrode in the GaAs.<sup>27,28</sup> This backgate bias or substrate bias, widely used in silicon inversion layers, changes the electric field in the depletion layer. The effect has been considered theoretically by Vinter<sup>2</sup> and will not be considered further here because it depends in part on the doping in the Ga<sub>1-x</sub>Al<sub>x</sub>As.

The results presented here give a sample of calculated results for an ungated GaAs-Ga<sub>1-x</sub>Al<sub>x</sub>As heterojunction on  $p$ -type GaAs, ignoring the effect of doping in the Ga<sub>1-x</sub>Al<sub>x</sub>As on the levels, which was found by Bastard<sup>29</sup> to be small. A calculation for accumulation layers in  $n$ -type GaAs is in general more difficult, except at low temperatures if the donors in the GaAs can be frozen out. In that case the fixed charge is determined by the compensating acceptor ions, leading to a very low value of  $N_d$ . Such calculations have been carried out by Ando<sup>1</sup> and Bastard<sup>25</sup> for GaAs-Ga<sub>1-x</sub>Al<sub>x</sub>As heterojunctions and by Bastard<sup>29</sup> for InP-(In,Ga)As heterojunctions. A few results for

small values of  $N_d$  have been given in Fig. 3 above.

Self-consistent calculations for quantum wells along the same lines as those presented here have been carried out, and results, including a comparison with a tight-binding calculation by Schulman<sup>30</sup> for a graded interface, are planned to be prepared for publication.

## V. DISCUSSION AND CONCLUSIONS

In this section we comment on some of the features exhibited by the results of this work, discuss some of the limitations of the calculations, and point out some directions for future work. Where comparison is possible, our results agree with those of Ando<sup>1</sup> who treated the interface somewhat differently and did not include image effects.

In many cases, calculations motivated primarily by device considerations have made rather severe approximations to estimate the energy levels. The most severe is to use the approximate energy for a triangular potential, in which the wave function is assumed to vanish at the interface and the field in the GaAs is taken to be a constant equal to its value at the interface. Alternatively, one can take the field to be the average of the interface field and the depletion field. Somewhat less severe is to use approximate results [given in Eqs. (16) and (17) of Ref. 26] that

still assume the wave function to vanish at the interface, but treat the band bending in the GaAs variationally. Table I compares the results of these approximations with results of the present self-consistent calculations, and also shows the sensitivity of the calculated results to some of the parameters. The first row of Table I gives the "best" calculated results, as presented in Fig. 2, and the fourth row from the bottom gives numerical results for a case with no image or exchange-correlation effects and with an infinite barrier height, the case with which the analytical approximations should be compared. The simpler results of the last three lines agree only roughly with the more accurate results, and give some feeling for the magnitude of the errors. The variational approximation gives the best results overall, but the assumption of infinite barrier height leads to energies that are higher than those for realistic barrier heights. A modified variational approach that allows the trial wave function to enter the barrier has been described by Ando.<sup>31</sup>

Although the present results are thought to give a fairly good description of the energy-level structure of single heterojunctions, they nevertheless have limitations which could become relevant in some cases. The use of the effective-mass approximation to describe the system omits contributions of higher-lying energy bands and associated effects near the interface. Some errors are also introduced by neglect of conduction-band nonparabolicity and the change in density-of-states effective mass associated with wave-function matching at the interface. The limitations of our simple local-density-functional approximation for effects of electron-electron interactions have already been discussed in Sec. III. These approximations could introduce errors of order 10% or more in the energies, with smaller errors expected in the energy differences. In addi-

tion, approximations in the numerical integrations could also introduce errors, but these should not exceed a percent or so if there have not been any errors in carrying out the calculations. With our present knowledge of GaAs-Ga<sub>1-x</sub>Al<sub>x</sub>As heterojunctions, these errors may well be overshadowed by the uncertainty in our knowledge of material parameters such as impurity concentrations and interface barrier heights.

Perhaps the main conclusion of this work is that some of the calculated results—especially the energy-level differences—are relatively insensitive to the values of many of the parameters that characterize the interface. On the other hand, they are sensitive to the net density of acceptors in the GaAs, which may not be easy to measure at levels near or below  $10^{15} \text{ cm}^{-3}$ . If one can establish confidence in the calculated results, then it may be possible to use spectroscopic measurements of level splittings<sup>28,32</sup> or transport measurements of the threshold for occupying the second subband<sup>23</sup> to determine this doping density, which can affect other properties of experimental interest such as charge balance between the GaAs and the Ga<sub>1-x</sub>Al<sub>x</sub>As and mobility of electrons in the channel. Note, however, that optical-absorption measurements and some Raman scattering measurements do not give the energy-level differences directly, but require corrections whose magnitude must be calculated.<sup>1,5</sup>

#### ACKNOWLEDGMENTS

We are indebted to G. Bastard, A. Pinczuk, J. N. Schulman, and B. Vinter for sending us unpublished results that bear on the subject of this paper, and to E. E. Mendez and P. J. Price for comments on the manuscript.

\*Present address.

<sup>1</sup>T. Ando, J. Phys. Soc. Jpn. **51**, 3893 (1982).

<sup>2</sup>B. Vinter, Surf. Sci. **142**, 452 (1984); Solid State Commun. **48**, 151 (1983).

<sup>3</sup>B. Vinter, Appl. Phys. Lett. **44**, 307 (1984).

<sup>4</sup>P. J. Price and F. Stern, Surf. Sci. **132**, 577 (1983).

<sup>5</sup>T. Ando, A. B. Fowler, and F. Stern, Rev. Mod. Phys. **54**, 437 (1982).

<sup>6</sup>F. Stern, Bull. Am. Phys. Soc. **28**, 447 (1983).

<sup>7</sup>F. Stern, Phys. Rev. B **17**, 5009 (1978).

<sup>8</sup>D. J. BenDaniel and C. B. Duke, Phys. Rev. **152**, 683 (1966).

<sup>9</sup>Nonparabolicity and density-of-states corrections associated with wave-function penetration into the barrier are ignored, except that we take an effective mass ( $m_c=0.07m_0$ ) slightly larger than the value at the conduction-band minimum in bulk GaAs.

<sup>10</sup>The grading function  $G(z)$  uses a different origin from the function  $S(z)$  used in Ref. 7, so that the center of the graded region now lies at  $z=0$ .

<sup>11</sup>P. Hohenberg and W. Kohn, Phys. Rev. **136**, B864 (1964); W. Kohn and L. J. Sham, *ibid.* **140**, A1133 (1965); L. J. Sham and W. Kohn, *ibid.* **145**, 561 (1966).

<sup>12</sup>A. R. Williams and U. von Barth, in *Theory of the Inhomogeneous Electron Gas*, edited by S. Lundqvist and N. H. March (Plenum, New York, 1983).

<sup>13</sup>T. Ando, Phys. Rev. B **13**, 3468 (1976).

<sup>14</sup>S. Das Sarma and B. Vinter, Phys. Rev. B **23**, 6832 (1981); **26**, 960 (1982); **28**, 3639 (1983).

<sup>15</sup>U. von Barth, in *The Electronic Structure of Complex Materials* (NATO Advanced Study Institute, Ghent, 1982).

<sup>16</sup>The electron density which enters here is only the density of the mobile carriers in the GaAs channel. In the effective-mass approximation, the effects of the bonding and core electrons are incorporated in the effective mass and dielectric constant.

<sup>17</sup>See Refs. 12 and 15 for extensive reference to work on the calculation of  $V_{xc}$ .

<sup>18</sup>L. Hedin and B. I. Lundqvist, J. Phys. C **4**, 2064 (1971).

<sup>19</sup>U. von Barth and L. Hedin, J. Phys. C **5**, 1629 (1972).

<sup>20</sup>D. C. Langreth and M. J. Mehl, Phys. Rev. Lett. **47**, 446 (1981).

<sup>21</sup>U. von Barth and R. Car (unpublished).

<sup>22</sup>S. Mori and T. Ando, Phys. Rev. B **19**, 6433 (1979); J. Phys. Soc. Jpn. **48**, 865 (1980).

<sup>23</sup>H. L. Störmer, A. C. Gossard, and W. Wiegmann, Solid State Commun. **41**, 707 (1981).

<sup>24</sup>N. T. Thang, G. Fishman, and B. Vinter, Surf. Sci. **142**, 266 (1984).

<sup>25</sup>G. Bastard, Surf. Sci. **142**, 284 (1984).

<sup>26</sup>F. Stern, Phys. Rev. B **5**, 4891 (1972).



<sup>27</sup>H. L. Störmer, A. C. Gossard, and W. Wiegmann, Appl. Phys. Lett. **39**, 493 (1981).

<sup>28</sup>Z. Schlesinger, J. C. M. Hwang, and S. J. Allen, Jr., Phys. Rev. Lett. **50**, 2098 (1983).

<sup>29</sup>G. Bastard, Appl. Phys. Lett. **43**, 591 (1983).

<sup>30</sup>J. N. Schulman (unpublished).

<sup>31</sup>T. Ando, J. Phys. Soc. Jpn. **51**, 3900 (1982).

<sup>32</sup>A. Pinczuk and J. M. Worlock, Physica **117B&118B**, 637 (1983).